Numerical Assessment of EEG Electrode Artifacts during EMF Exposure in Human Provocation Studies

Maria Christopoulou*, Orestis Kazasidis, and Konstantina S. Nikita

Biomedical Simulations and Imaging Unit (BIOSIM)
School of Electrical and Computer Engineering, National Technical University of Athens
9 Iroon Polytechniou, Zografou Campus, 15780, Athens, Greece
mchrist@biosim.ntua.gr, orestis.kaza@gmail.com,
knikita@cc.ece.ntua.gr

Abstract. The paper presents the numerical evaluation of the electroencephalogram (EEG) electrode artifacts that are caused during exposure to electromagnetic fields (EMF), in volunteers study. The scope of the study is to differentially present the electromagnetic (EM) power absorption and local Specific Absorption Rate (SAR) distribution, with and without the electrodes. Versions of two basic exposure scenarios are evaluated: flat layered tissue phantom and anatomical head model exposed to plane wave or patch antenna radiation at operating frequency of 1966 MHz. Finite Difference Time Domain (FDTD) method is used in order to model the computational domain. E-field distributions and SAR values are calculated. The electromagnetic power absorption by the brain tissues is correlated with the presence of the EEG electrodes and the relative positioning of their leads. Results conclude in significant alternations in EM power absorption, E-field and SAR distributions, due to the co-polarization between the leads and the E-field. Concerning the realistic scenario, the presence of 32 electrodes and their leads enhances (11% without and 12.3% with electric contact) the $psSAR_{10g}$, comparing to the reference simulation.

Keywords: Specific Absorption Rate (SAR), Finite Difference Time Domain (FDTD) method, numerical dosimetry, electroencephalogram (EEG), electrode, human provocation study.

1 Introduction

In human provocation studies, the electromagnetic (EM) exposure prior the sleep electroencephalogram (EEG) [1] or the Event Related Potentials (ERP) recordings is often performed with the volunteers having the EEG cap already worn, in order to minimize time between exposure and sleep onset or cognitive task initiation. In [2] the Specific Absorption Rate (SAR) enhancement has been numerically evaluated due to simultaneous MRI and EEG recordings. Simulations have been conducted for 128 MHz-3 Tesla and 300 MHz-7 Tesla with 16, 31, 62 and 124 electrodes. Hamblin *et al.*

* Corresponding author.

S. Müller Arisona et al. (Eds.): DUMS, CCIS 242, pp. 408–415, 2012.

[3] have experimentally and numerically assessed the effect of two 64-electrodes EEG caps on the SAR values for 900 MHz. The main outcome of the study included reduction of peak spatial SAR averaged over 10g ($psSAR_{10g}$) due to the presence of electrode leads. Lately [4]-[5], the shielding effect, the SAR alternation and E-field artifacts have been evaluated for UMTS-like exposure, according to the reported exposure scenario.

This paper is part of the numerical dosimetry for a human study, according to published guidelines for provocation studies [6]. The volunteers study is a collaboration between the Biomedical Simulations and Imaging (BIOSIM) Unit and the University Mental Health Research Institute, aiming at the assessment of potential alternations in electroencephalogram (EEG) and event related potentials (ERP) recordings during acoustic stimuli, due to exposure to UMTS-like EM signal. Before EEG and ERP recordings, the subjects are exposed for 30 min to EM radiation, having the EEG cap already worn. In this paper, the EEG electrodes artifacts are numerically evaluated, concerning the power absorption, the local SAR and E-field distribution. The electrodes that will be used during the human study are modeled and the evaluation is carried out with i) flat phantom and ii) realistic head model.

2 Materials and Methods

Two basic exposure scenarios, including modifications, are numerically modeled and simulated: a) flat layered phantom with one electrode attached and b) anatomical head model with an EEG cap of 32 electrodes attached. Both scenarios are comparatively assessed with the corresponding reference ones, without electrodes. The used operating frequency is 1966 MHz, corresponding to UMTS operating frequency band. Apart from a plane wave, the numerical models are exposed to the radiation of the wideband patch antenna SPA 2000/80/8/0/V (Huber & Suhner), placed at x=-180 mm separation distance. Measurements data of the antenna operation characteristics are in agreement with the corresponding simulated ones and they are both presented in [7].

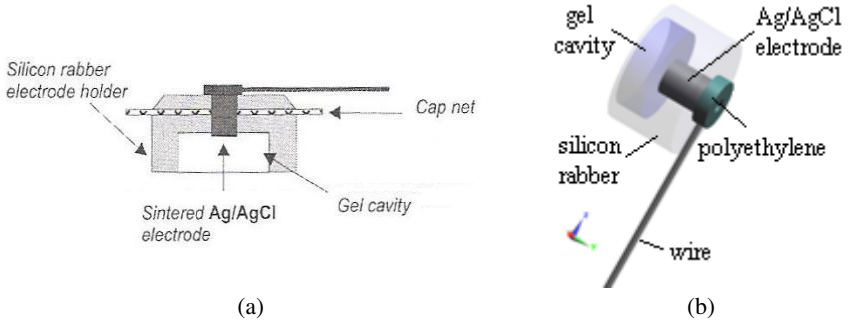

Fig. 1. Description of the electrode's structure: a) real and b) numerical model

Fig. 1(a) illustrates the real model of the electrodes that are attached to Softcap (Spes Medica) and will be used in the volunteers study. Fig. 1(b) illustrates the derived numerical model, where the Ag/AgCl electrode (PEC), silicon rabber electrode holder (ε_r=3.2, σ=0.0265 Si/m), gel cavity (air) and the polyethylene

connection (ε_r=2.25, σ=0.0005 Si/m), between the electrode and the lead (PEC) are separately denoted. The electrode lead is covered by PVC (ε_r=2.8, σ=0.019 Si/m). In order to simulate the electric contact between the skin and the electrode, gel cavity is selectively characterized as PEC. Computational dosimetry is conducted for flat layered tissue phantom and anatomical head model using the SEMCAD-X v14.2 software (SPEAG, Zurich, Switzerland) and the Finite Difference Time Domain (FDTD) method [8].

2.1 Flat Layered Phantom Exposure Scenario

For preliminary evaluation, a flat phantom with one electrode attached, is used. The flat phantom is structured in eight (8) layers [4] and it is considered to simulate the head biological tissues' sequence, from the external tissue to the inner one, as it is tabulated in Table 1. Table 1 also includes the dielectric properties of the tissues at 1966 MHz [9] and the thickness that is used, according to anatomy information [10].

Table 1. Thickness and dielectric properties (at operating frequency 1966 MHz) of the biological tissues in flat layered phantom

biological tissue	thickness (mm)	ε_r	σ (S/m)	ρ (kg/m^3)
dry skin	2	38.62	1.25	1100
fat (not infiltrated)	1	5.33	0.08	916
muscle	4	53.33	1.43	1041
cortical bone	6	11.67	0.30	1990
dura matter	1	42.67	1.40	1013
CSF	2	66.96	3.05	1007
grey matter	4	49.76	1.49	1039
white matter	150	36.78	0.99	1043

The flat layered phantom exposure scenario is illustrated in Fig. 2(a). One electrode with its lead is attached to the external tissue (dry skin). The electric contact between Ag/AgCl electrode and skin is modeled by altering the gel cavity dielectric properties and height. The electrode lead is set differently in order to be co- and cross-polarized with the incident E-field. A plane wave at 1966 MHz or the patch antenna at distance x=-180 mm are both used, as electromagnetic sources. The computational grid consists of ~24 Mcells and the simulation time is set to 20 periods.

2.2 Anatomical Head Exposure Scenario

The proposed anatomical head exposure scenario is illustrated in Fig. 2(b). As realistic head model, 'Ella' from Virtual Family [11] is used, corresponding to MRI data of a 26 year old adult woman. 'Ella' model has a resolution of $0.5\times0.5\times0.5\text{mm}^3$ and consists of 41 head structures. 32 electrodes (with and without their leads) are mounted on the numerical head, according to 10-20 extended system [12]. The leads are placed as horizontally as possibly, in order to minimize the alternations in E-field

distribution and the enhancement in SAR values [5]. Only the patch antenna is used, simulating the real experimental scenario, during the human provocation study. The center of the antenna is placed at (x,y,z)=(-180,0,42) mm, considering as (0,0,0), the right ear canal. The computational grid consists of 41-95 Mcells, depending on the exposure scenario ((a) reference, (b) with electrodes, (c) with electrodes and leads), and the simulation time is set to 35 periods.

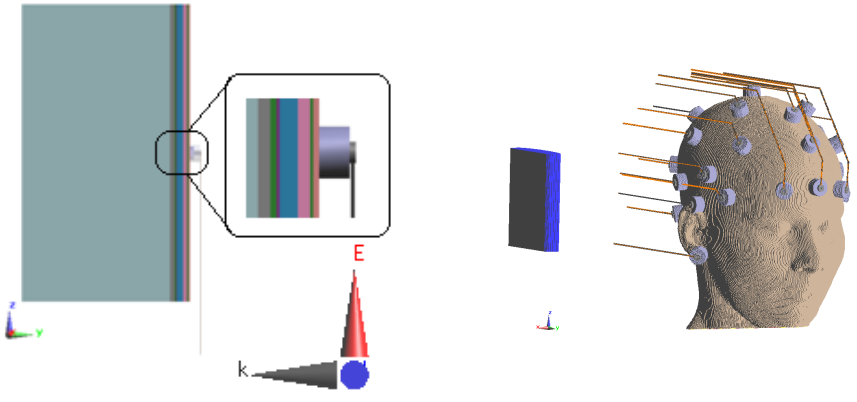

(a) (b)

Fig. 2. Geometry of the proposed exposure scenarios at 1966 MHz: a) flat layered phantom with one electrode and lead attached, exposed to plane wave (co-polarization), b) realistic head with 32 electrodes and leads attached-according to 10-20 system, exposed to irradiation of the patch antenna.

3 Simulation Results

All the results are differentially presented as compared to the reference simulations, i.e. the corresponding ones without the presence of the electrodes and their leads. All results are normalized to 1 W input power. The gel cavity is generally simulated as air, except the worst case scenario that is presented for anatomical head. In this section, results of both exposure scenarios are presented.

3.1 Flat Layered Phantom Exposure Scenario

For the case of the flat layered phantom exposed to plane wave, the surface E_{rms}-field distribution is illustrated in Fig. 3. The results confirm that the co-polarization of the electrode lead can cause significant distortion in the E-field distribution, as previous studies [4]-[5] emphasize. Additionally, there is an E-field enhanced area, parallel to the electrode lead, between two regions of significantly low values. In case of cross-polarization (Fig. 3(c)), there is a slight amplification in the center of the flat phantom, corresponding to the electrode. This amplification is local and almost superficial and it is restricted to the external layers of the phantom (up to 10 mm). The presence of the lead has no result in the E-field distribution.

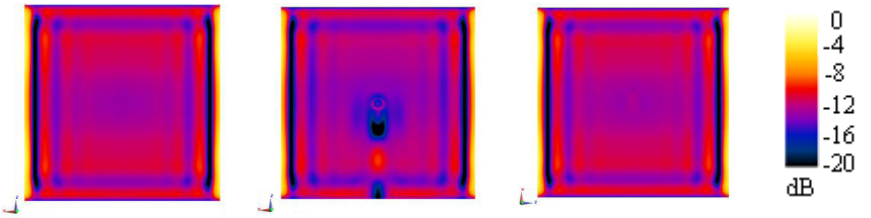

Fig. 3. Surface E_{rms}-field distribution for the a) reference simulation, b) co- and c) cross-polarization. All values are normalized to 14.5 V/m (0 dB).

Additionally, the $psSAR_{1g}$ [13] is calculated for each exposure scenario. Comparing to the reference simulation (0.2459 W/kg), an increase of over 11% in the co-polarization (0.2629 W/kg) and a slight decrease of 1% in the cross-polarization (0.2339 W/kg) are calculated for the $psSAR_{1g}$ values.

For the case of the flat layered phantom exposed to the SPA 2000/80/8/0/V patch antenna irradiation, the local SAR distribution at x=0 mm and z=0 mm, where the electrode has been placed, is comparatively illustrated in Fig. 4. The results confirm that the local SAR distribution presents almost the same pattern for the reference and the cross-polarization scenario. In the co-polarization scenario, the presence of the electrode lead causes SAR attenuation of approximately 15 dB in selected tissues, such as dry skin. Comparing the local SAR calculated for each biological tissue, dry skin, muscle and CSF are the ones that absorb the most of the radiated EM power. This is related to their comparatively large values of electrical conductivity as well as their small distance from the EM source.

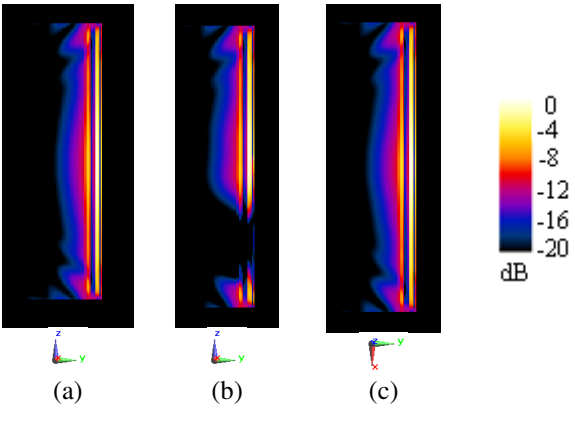

Fig. 4. Local SAR distribution for the a) reference simulation (x=0 mm) b) co- (x=0 mm) and c) cross-polarization (z=0 mm). All values are normalized to 0.6 W/kg (0 dB).

3.2 Anatomical Head Exposure Scenario

In case of the anatomical head model exposed to the radiation of the patch antenna, E-field distribution and SAR values in each brain structure are assessed. Fig. 5

illustrates the E-field distribution at y=0 slice for (a) reference, (b) with electrodes and (c) with electrodes and leads simulations. Enhancement of the E-field values along the leads is obvious at both sides of the head. Comparing the three simulations, the E-field distribution in the head remains almost unchanged.

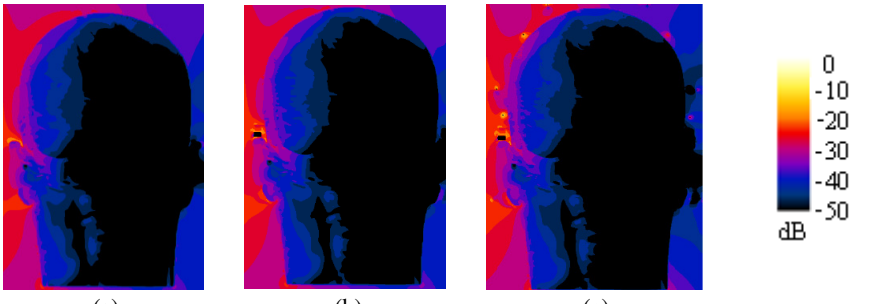

Fig. 5. E-field distribution at the y=0 slice. Simulation (a) reference, (b) with electrodes, (c) with electrodes and leads. All values are normalized to 10^3 V/m (0 dB).

In order to simulate the worst case scenario of electric contact between the electrode and the skin, the gel cavity for each of the 32 electrodes is characterized as PEC. Therefore, Fig. 6 compares the local SAR surface distribution for the following simulations: (a) reference, (c) electrodes and leads, with gel cavity characterized as air and (d) electrodes and leads, with gel cavity characterized as PEC. It is obvious that when there is no electric contact between the skin and the electrode, no significant difference in the local SAR surface distribution is reported. In (d) scenario, the characterization of the gel cavity as PEC leads to attenuation of the SAR values below the cavity and amplification of the EM absorbed power around the electrode.

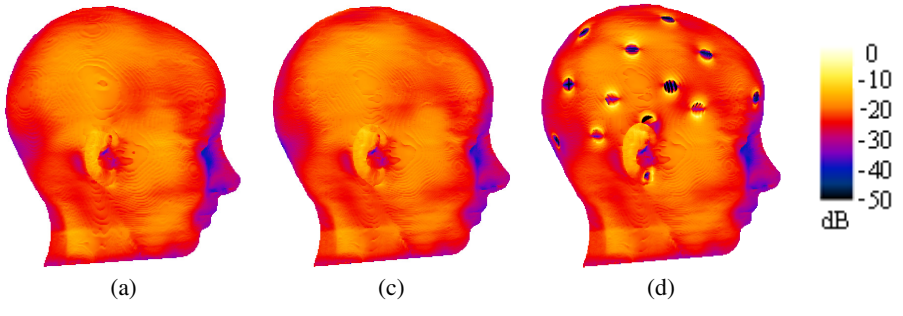

Fig. 6. Local SAR surface distribution. Simulation (a) reference, (c) with electrodes and leads (gel cavity: air), (d) with electrodes and leads (gel cavity: PEC). All values are normalized to 50.37 W/kg (0 dB).

Additionally, the $psSAR_{1g/10g}$ [13] and the averaged SAR over the whole mass of selected brain structures are calculated for all simulations. Comparing to the reference simulation (0.5015 W/kg), an increase of 11% in the (c) scenario simulation (0.5569

W/kg) and 12.3% in the (d) scenario (0.5632 W/kg) are calculated, correspondingly for the head $psSAR_{10g}$ values. Indicatively, Table 2 includes the $psSAR_{1g}$ and averaged SAR calculations in selected brain structures and head for both hemispheres, comparing (a), (c) and (d) simulation scenarios. Concerning the $psSAR_{1g}$, the maximum alternation (45% decrease) is noticed in thalamus for simulation (d), comparing to the reference one. For averaged SAR, the corresponding maximum alternation (44% decrease) is assessed also in thalamus for simulation (d).

Table 2. $psSAR_{1g}$ and averaged SAR values calculated in selected brain structures and head for (a) reference, (c) electrodes with leads and (d) electrodes with leads and gel cavity as PEC simulations.

brain structure or head	$psSAR_{1g}$ (W/kg)			Avg. SAR (W/kg)		
	(a)	(c)	(d)	(a)	(c)	(d)
grey matter	0.312	0.308	0.360	0.036	0.036	0.030
white matter	0.164	0.163	0.153	0.021	0.029	0.018
thalamus	0.022	0.022	0.012	0.009	0.006	0.005
midbrain	0.013	0.012	0.008	0.004	0.004	0.003
averaged brain w/o CSF	0.297	0.291	0.351	0.028	0.029	0.024
head	1.812	1.819	2.320	0.042	0.043	0.040

4 Conclusions

A detailed numerical evaluation for EEG electrodes artifacts is described in this paper. Versions of two basic exposure scenarios are evaluated: i) flat layered phantom with one electrode attached and ii) realistic head model with 32 electrodes attached. Results conclude in significant alternations in EM power absorption, E-field and SAR distributions, due to the co-polarization between the leads and the E-field. Concerning the realistic scenario, the use of 32 electrodes and their leads results in an 11% increase (12.3% with electric contact) of the head $psSAR_{10g}$, comparing to the reference simulation. Future work can be focused on altering the number of the electrodes and orientation of their leads on the realistic head. This study along with variation and uncertainty numerical evaluation completes the full numerical dosimetry assessment that should always precede a human provocation study.

References

1. Huber, R., Schuderer, J., Graf, T., Jütz, K., Borbély, A.A., Kuster, N., Acherman, P.: Radio frequency electromagnetic field exposure in humans: estimation of SAR distribution in the brain, effects on sleep and heart rate. Bioelectromagnetics 24, 262–276 (2003)
2. Angelone, L.M., Potthast, A., Segonne, F., Iwaki, S., Belliveau, J.W., Bonmassar, G.: Metallic electrodes and leads in simultaneous EEG-MRI: Specific Absorption Rate (SAR) simulation studies. Bioelectromagnetics 25, 285–295 (2004)

3. Hamblin, D.L., Anderson, V., McIntosh, R.L., McKenzie, R.J., Wood, A.W., Iskra, S., Croft, R.J.: EEG electrode caps can reduce SAR induced in the head by GSM 900 mobile phones. IEEE Trans. Biomed. Eng. 54, 914–920 (2007)
4. Murbach, M., Kuehn, S., Christopoulou, M., Christ, A., Achermann, P., Kuster, N.: Evaluation of Artifacts by EEG Electrodes during RF Exposures. In: BioElectromagnetics Annual Meeting (BioEM), Davos, Switzerland, June 14-19 (2009)
5. Schmid, G., Cecil, S., Goger, C., Trimmel, M., Kuster, N., Molla-Djafari, H.: New head exposure system for use in human provocation studies with EEG recording during GSM900 and UMTS-like exposure. Bioelectromagnetics 28, 636–647 (2007)
6. Kuster, N., Schuderer, J., Christ, A., Futter, P., Ebert, S.: Guidance for Exposure Design of Human Studies Addressing Health Risk Evaluations of Mobile Phones. Bioelectromagnetics 25, 524–529 (2004)
7. Murbach, M., Christopoulou, M., Crespo-Valero, P., Achermann, P., Kuster, N.: System to Study CNS Responses of ELF Modulation and Cortex versus Subcortical RF Exposures. Bioelectromagnetics (2012) (accepted for publication)
8. Taflove, A.: Computational Electromagnetics-The Finite Difference Time Domain Method. Artech House Publishers, Boston (1995)
9. Gabriel, S., Lau, R.W., Gabriel, C.: The dielectric properties of biological tissues: III. Parametric models for the dielectric spectrum of tissues. Phys. Med. Biol. 41, 2271–2293 (1996)
10. Farkas, L.G.: Anthropometry of the head and face, App A, 2nd edn., p. 244. Raven Press, New York (1994)
11. Christ, A., Kainz, W., Hahn, E.G., Honegger, K., Zefferer, M., Neufeld, E., Rascher, W., Janka, R., Bautz, W., Chen, J., Kiefer, B., Schmitt, P., Hollenbach, H.P., Shen, J., Oberle, M., Szczerba, D., Kam, A., Guag, J.W., Kuster, N.: The Virtual Family—development of surface-based anatomical models of two adults and two children for dosimetric simulation. Phys. Med. Biol. 55, N23–N38 (2010)
12. Rowan, A.J., Tolunsky, E.: Primer of EEG with a Mini-Atlas. Elsevier Science, United States of America (2003)
13. IEEE: Recommended Practice for Measurements & Computations of RF EM fields with Respect to Human Exposure to Such Fields. IEEE Standard C95.3-2002 (2002)